Airborne lidar for simultaneous measurement of column CO_2 and water vapor in the atmosphere

Upendra N. Singh*[a], Mulugeta Petros[b], Tamer F. Refaat[b],
Charles W. Antill[b], Ruben Remus[b] and Jirong Yu[b]
[a]NASA Engineering and Safety Center, NASA Langley Research Center, Hampton, VA, USA;
[b]Remote Sensing Branch, NASA Langley Research Center, Hampton, VA, USA

ABSTRACT

The 2-micron wavelength region is suitable for atmospheric carbon dioxide (CO_2) measurements due to the existence of distinct absorption feathers for the gas at this particular wavelength. For more than 20 years, researchers at NASA Langley Research Center (LaRC) have developed several high-energy and high repetition rate 2-micron pulsed lasers. This paper will provide status and details of an airborne 2-micron triple-pulse integrated path differential absorption (IPDA) lidar. The development of this active optical remote sensing IPDA instrument is targeted for measuring both CO_2 and water vapor (H_2O) in the atmosphere from an airborne platform. This presentation will focus on the advancement of the 2-micron triple-pulse IPDA lidar development. Updates on the state-of-the-art triple-pulse laser transmitter will be presented including the status of seed laser locking, wavelength control, receiver telescope, detection system and data acquisition. Future plans for the IPDA lidar system for ground integration, testing and flight validation will also be presented.

Keywords: Active remote sensing, carbon dioxide, water vapor, DIAL, IPDA lidar, triple-pulse laser

1. INTRODUCTION

Recently, an airborne 2-μm high-energy, double-pulse integrated path differential absorption (IPDA) lidar have been integrated and validated at NASA Langley Research Center (LaRC) for atmospheric carbon dioxide (CO_2) measurements [1]. This double-pulse IPDA was tuned around the CO_2 R30 strong absorption line at 2050.9670 nm, which is optimum for lower tropospheric weighted column measurements. Airborne field experiments were conducted to quantify and characterize instrument capabilities, sensitivity and bias errors by comparison to performance models. In one experiment, the 2-μm IPDA lidar measurements were validated by comparison to airborne CO_2 flask air-sampling measurements conducted by the NOAA Earth System Research Laboratory. The IPDA CO_2 column measurements compare well with model-driven, near-simultaneous air-sampling measurements from NOAA aircraft at different altitudes. CO_2 differential optical depth measurement of 1.0054±0.0103 was retrieved from a 6-km altitude with 4-GHz on-line operation and 10 sec shot average. As compared to CO_2 weighted-average column dry-air volume mixing ratio of 404.08 ppm, derived from air sampling, the double-pulse IPDA measurement resulted in a value of 405.22±4.15 ppm with 1.02% uncertainty and 0.28% systematic bias [1]. IPDA ranging, a byproduct of pulsed systems, resulted in a measurement uncertainty of less than 3 m. In another airborne experiment, off-off-line testing was conducted with fixed instrument settings to evaluate the IPDA systematic and random errors [1]. CO_2 optical depth measurement uncertainty of 0.0918 compares well with the predicted value of 0.0761. Analysis showed an altitude-independent differential optical depth offset of 0.0769. Results were consistent between both flights. Sensitivity analysis of environmental systematic errors correlates this additional bias to water vapor (H_2O). Atmospheric H_2O results in significant interference in CO_2 measurement due to the strong absorption characterizes at 2-μm. This is a common problem in CO_2 measurement in the IR spectral region which limits the measurement sensitivity. In addition, knowledge of H_2O distribution is essential for obtaining the dry-air number density for converting measured CO_2 optical depth, the primary IPDA product, into dry-air weighted average column volume-mixing ratio [1-5].

To address this technical issue, a 2-μm triple-pulse IPDA is currently under development at NASA LaRC through continual support from the NASA Earth Science Technology Office (ESTO) [6]. This triple-pulse IPDA will allow simultaneous and independent measurement of H_2O and CO_2 optical depths from an airborne platform [7]. This system is a technological update to the knowledge gathered through the 2-μm CO_2 double-pulse IPDA lidar system. The triple-pulse IPDA lidar under evaluation is a direct detection system based on a state-of-the-art high repetition rate, high-energy, triple-pulse, 2-μm laser transmitter. In this paper, the development status of critical instrument component will be detailed and challenges

will be addressed. This includes updates on the state-of-the-art triple-pulse laser transmitter, the status of seed laser locking, wavelength control, receiver telescope, detection system and data acquisition upgrades. This novel technique allows measurement of the two most dominant greenhouse gases, simultaneously and independently, using a single instrument. Therefore, the design of this airborne triple-pulse IPDA lidar instrument enables technology development for future space-based system for global CO_2 measurement, while reducing risk, cost, size, volume, mass and development time of required sensor [8].

2. AIRBORNE TRIPLE-PULSE IPDA TECHNIQUE

The IPDA technique measures the total integrated column content from the instrument to the hard target. For an airborne nadir IPDA, schematically shown in figure 1, Earth's surface is the hard target and the total column content will be weighted depending on the transmitted wavelengths [9]. For the 2-μm triple-pulse IPDA, the wavelength of each of the transmitted pulses is tuned and locked independently in the neighborhood of the CO_2 R30 line. The three pulses are generated using a single pump pulse, with energies that is controlled by the Q-switch timing. This event repeats every 20 msec, equivalent to 50 Hz repetition rate, with pulse separation of 150-200 μsec. This short pulse separation results in higher than 95% laser footprint overlap at the surface from 4 km altitude. The operational wavelengths of the pulses are selected to reduce H_2O interference and provide optical depth conversion estimates by measuring H_2O simultaneously and independently while measuring CO_2 [10]. This triple-pulse IPDA measurement concept is presented in figure 2. The figure presents the vertical integrated optical depth spectral profile for CO_2 and H_2O around the CO_2 R30 line [1]. The optical depths were derived using HITRAN database for absorption line parameters, assuming Voigt profile, and the US standard atmosphere model for meteorological and molecular profiles [7]. The presented optical depth integration upper limit is based on 8 km airborne altitude, assuming a small aircraft such as the NASA B-200. Sea level is considered for the lower limit. The H_2O absorption peak, located at 2050.5322 nm, coincides close to CO_2 absorption minima between R30 and R32 lines and away from the R32 peak. The unique tuning and locking capabilities of the 2-μm laser transmitter allow proper selection of the IPDA operating wavelengths. The principle of wavelength selection for this IPDA instrument is demonstrated in the same figure. The CO_2 on- and off-line wavelengths are selected around the R30 line, so that both would have similar H_2O absorption (lower horizontal line). This minimizes the H_2O interference on the CO_2 measurements. Similarly, the H_2O on- and off-line wavelengths are selected around the absorption peak such that CO_2 interference is minimized on the H_2O measurement (upper horizontal line). Molecular interference minimization, through wavelength selection, results in independent measurement. However, CO_2 and H_2O measurements share the same wavelength (i.e., the same pulse) for the on-line and off-line, respectively. This allows achieving simultaneous measurement of both gases with triple pulses rather than quadruple pulses almost independently while avoiding interference from each other. To achieve this objective, the operating wavelengths of the first, second and third pulses are set to 2050.5094, 2051.0590 and 2051.1915 nm, respectively, which are equivalent to 32, -6 and -16 GHz offsets for the R30 line center at 2050.967 nm. Transmitted energies of 50, 15 and 5 mJ for the first, second and third pulses, respectively, are projected [7].

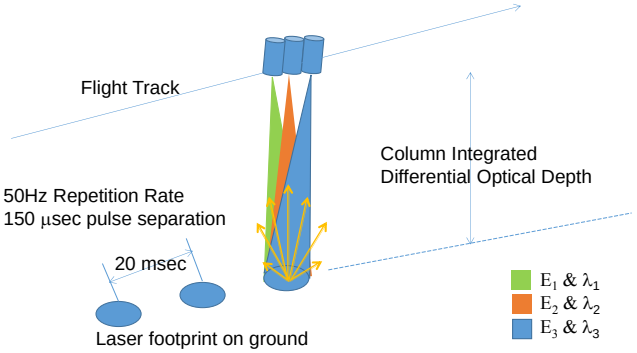

Figure 1. Airborne nadir 2-μm triple-pulse IPDA lidar concept. Each pulse is generated with different wavelength and energy. The three pulses are transmitted every 20 msec, equivalent to 50 Hz repetition rate. Pulse separation of 150-200 μsec results in higher than 95% laser footprint overlap at 4 km altitude.

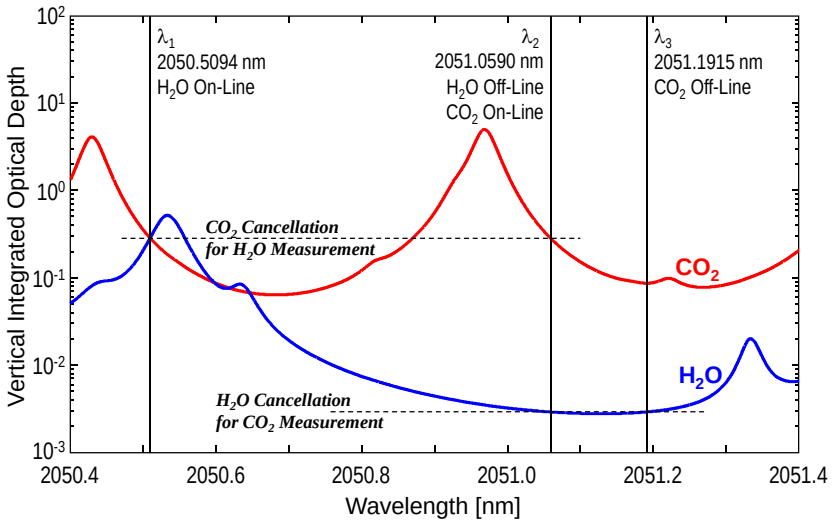

Figure 2. Comparison of the CO_2 and H_2O integrated optical depths derived using the HITRAN data base for line parameters and US Standard atmosphere model for metrological and molecular profiles. Vertical lines mark the instrument selected wavelengths for the three laser pulses, for simultaneous and independent CO_2 and H_2O measurements.

3. TRIPLE-PULSE TRANSMITTER

The triple-pulse IPDA laser transmitters is based on the Ho:Tm:YLF high-energy 2-µm pulsed laser technology [8]. The generated 2-µm laser beam is transmitted coaxially with the receiver telescope after beam expansion. Energy monitors will be installed inside the laser enclosure to detect and measure the energy of each of the transmitted pulses [11]. The exact wavelengths of the three pulses are controlled by a wavelength control unit.

3.1 Triple Pulse Laser Development

The 2-µm triple-pulse IPDA laser transmitters is based on a solid state Thulium (Tm) and Holmium (Ho) co-doped crystal. The crystal is end pumped by fiber coupled AlGaAs diode arrays at 792 nm. The long lifetime of this laser material allows the generation of multiple Q-switch pluses using a single pump. The IPDA laser transmitter is designed to emit three consecutive pulses within short intervals to mitigate the effect of the surface reflection difference between the different operating wavelength pulses on the precision of the measurement [8]. Figure 3 shows the laser timing control (LTC) unit. This unit controls several aspects of the laser operation that allows the user to change settings through a graphical user interface (GUI). The operation and control of this unit was tested successfully using the double-pulse IPDA. This unit is three times lighter than what was developed in double-pulsed IPDA. All laser required electronics were integrated in the LTC box. These include pulse timing electronics, seeding electronics, laser detectors amplifiers, interfacing and diagnostics. A single-shot event starts with the pump pulse that enables the pump diode. Q-switch triple-trigger, relative to the pump pulse, produces three successive 2-µm laser pulses with relatively controlled energies and pulse-widths. The laser is injection seeded with the three different wavelengths by ramp-and-fire method, which allows the Q-switch fire signal when the oscillator length is an integer multiple of the seed wavelength. The objective is to set the first pulse (32 GHz) to higher energy of 50 mJ to accommodate H_2O high variability absorption loss through on-line tuning. The second pulse (-6 GHz) is set to lower energy of 15 mJ to accommodate CO_2 absorption loss. In addition the same pulse would act as the H_2O offline wavelength. The third pulse (-16) with the lowest energy setting of 5 mJ would serve as the CO_2 off-line. These settings can be changed depending on the required measurement objective. For example, both the 50 and 15 mJ pulses could be tuned to two different CO_2 on-line wavelengths resulting in simultaneously measuring the gas with different weighting functions. Figure 4 compares the total generated 2-µm pulse energy variation with the pump laser energy for single- double and triple-pulse operation. These measurements were conducted using thermal energy meter that may under estimate the total energy for multi-pulses [11-12]. It is projected to enhance multi-pulse energy measurements using quantum based detection, similar to the double-pulse IPDA. Heat accumulation is a major challenge limiting the 2-µm output energy and can result in crystal damage. Thermal analysis was conducted to investigate the proper heat

dissipation rate out of the laser crystal, as shown in figure 5. Different laser crystal configurations were investigated that included different Tm doping concentrations, single and double-end pumping, different dimensions and un-doped diffusion bonding. A prototype oscillator with triple pulsing capability was demonstrated and final thermal analysis and alignment optimization is currently on going to increase the output energy [6].

Figure 3. 2-µm laser timing diagram (left) generated by the integrated laser timing control (LTC) unit (right). An event starts with the pump pulse that energizes the crystal. Q-switch triple-trigger, relative to the pump pulse, produces three successive 2-µm laser pulses. Q-switch is enable during the laser cavity length adjustment.

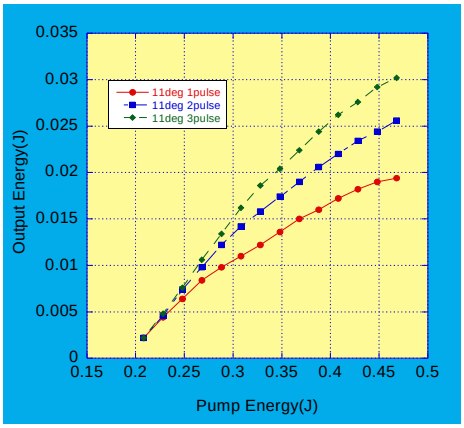

Figure 4. Total generated 2-µm pulse energy variation with the pump laser energy for single- double and triple-pulse operation. Maximum output energy of 30 mJ was successfully achieved with triple-pulse operation. Work efforts are currently focused to increase this energy to 70 mJ.

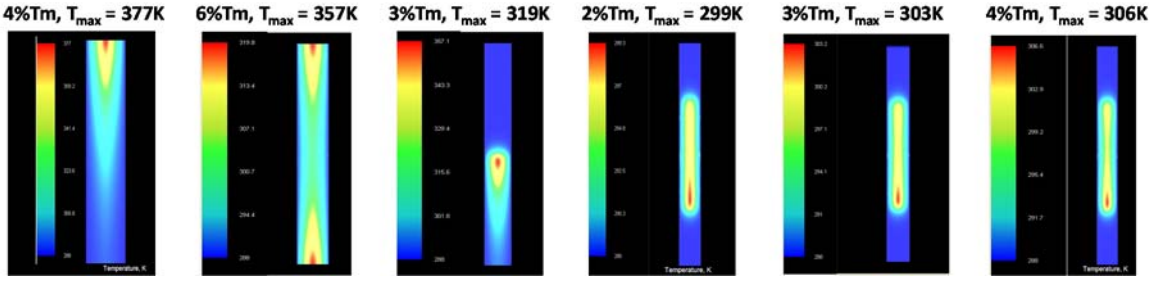

Figure 5. Thermal analysis conducted to investigate the temperature distribution and proper heat dissipation rate out of the laser crystal. Head load depends on thulium (Tm) doping concentration, single or double-end pumping and un-doped diffusion bonding.

3.2 Wavelength Control

The wavelength control unit generates the seeding of the 2-μm triple-pulse laser with a required accuracy less than ±1 MHz [7]. This unique wavelength control uses a single seed semiconductor laser at 2-μm. The fiber-coupled seed laser was developed at NASA Jet Propulsion Laboratory (JPL) [13]. The unit provides any frequency setting within 35 GHz from the CO_2 R30 line center reference. The wavelength control unit includes several electronic, optical and electro-optical components. The setup for the CO_2 absorption line center locking is shown in figure 6. Laser diode driver and control and center line locking electronics were design, integrated and test at NASA LaRC, as shown in figure 7. The seed laser output is split into 10% and 90% beams. The 90% beam is modulated with a 200 MHz electro-optics modulator. Center line locking electronics drives the modulator to generate two wavelengths offsets ±2.78 pm from CO_2 line center. The modulated output is collimated and applied to a CO_2 gas cell. The cell output is detected and fed back to the center line locking electronics to sense the error signal. Center line locking unit is capable of operating in a free-running mode or locked mode, as shown in figure 8. In free-running mode the center line locking does not control the laser diode driver, which is useful for diagnostics through the error and detector monitors. In locked-mode, the center line locking controls the laser diode current driver, through the servo signal, to precisely lock the device output wavelength. Figure 8 compares the error signal for unlocked and locked seeding. Statistical analysis of the locked center line wavelength resulted in ±650.1 kHz jitter, which is better than the projected jitter of ±1 MHz, as shown in the same figure [14]. Once the center line is locked, the 10% beam is passes through another unit to produce the required side lines within 2 to 35 GHz from the center reference wavelength. These lines are set to the 32, -6 and -16 GHz in reference to the R30 line. Figure 9 shows the side line seeding wavelength generation results.

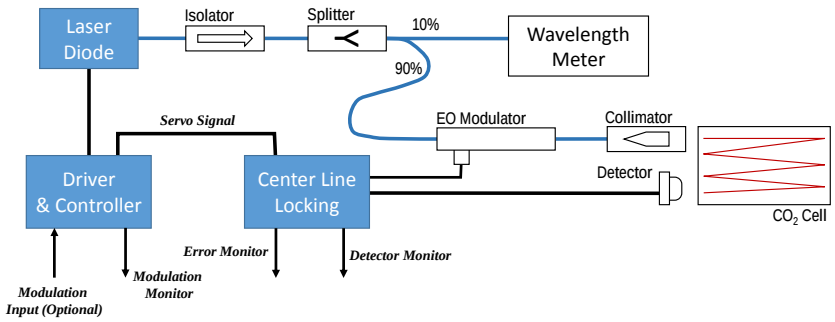

Figure 6. Setup of the CO_2 absorption line center locking. Center line locking electronics drives a 200 MHz EO modulator to generate two wavelengths offsets. Modulated output is collimated and applied to the CO_2 cell, the output of which is detected and feedback to center line locking electronics, which is capable of operating in a free-running mode or locked mode, as demonstrated in figure 8, through servo enable signal.

Figure 7. Packaged laser diode enclosure and laser diode current driver and temperature controller units and center line locking units. Duplicate electronics were integrated for two devices, including power supplies and the CO_2 cell detector. Laser diode electronics enclosures sizes are 6.5×6×4 and 16.5×11×3 cm^3, respectively.

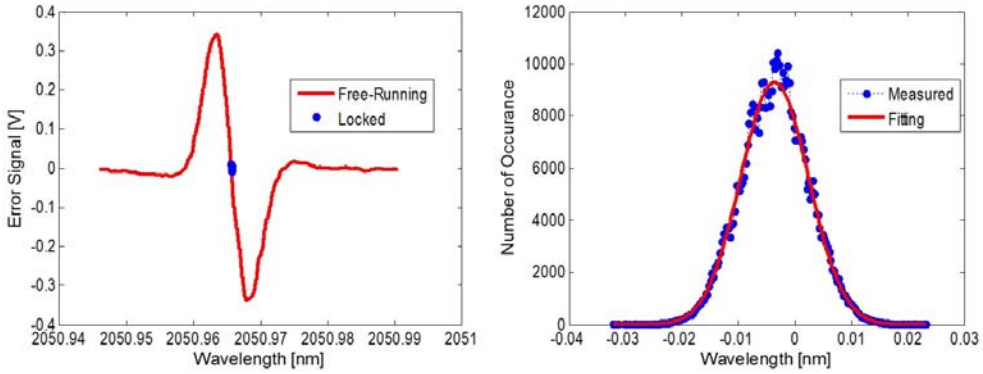

Figure 8. Comparison of the error signals for the center line locking free-running and locked modes (left). Statistical analysis and Gaussian distribution fitting (right) of the locked wavelength. Results indicated wavelength mean and standard deviation of 2050.966967 nm and 0.00913 pm, respectively. Standard deviation translates to ±650.1 kHz wavelength jitter.

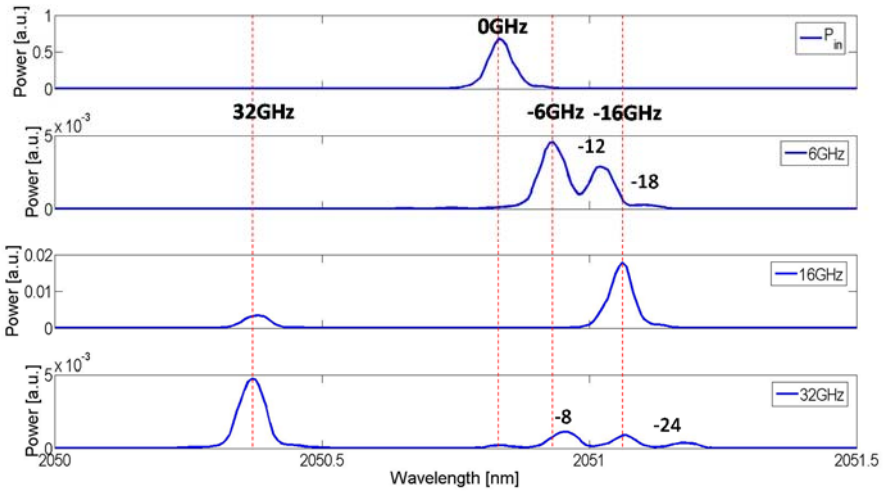

Figure 9. Optical spectrum analyzer records for the seeding wavelength generation relative to the locked center line at 0 GHz, which was rejected successfully. The -6 GHz seeding results in a second harmonic that is within the system bandwidth. Cross talk was observed between the -16 GHz second harmonic and the 32 GHz sub-harmonics.

4. IPDA RECEIVER

The 2-μm triple-pulse IPDA lidar receiver, shown schematically in figure 10, consists of a telescope that focuses the radiation onto aft-optics that collimates and filters the radiation before splitting. The beam splitter generates two optical channels. The first optical channel is a high signal channel with 90% of the radiation applied to a focusing lens on to a 300 μm diameter InGaAs pin detector (Hamamatsu; G5853). The detector output is amplified through a trans-impedance amplifier (TIA). The TIA has the capability to adjust the feedback gain and detection bandwidth. This detection channel is an exact replica to the double-pulse IPDA instrument. Since this channel was demonstrated for CO_2 measurements, it is included as a reference. The second low signal channel, with 10% radiation, is focused down to accommodate any other detector for IPDA lidar detection investigation. Currently, this channel is planned to be used for a newly-developed detection system by NASA Goddard Space Flight Center (GSFC) that is based on electron-initiated avalanche photodiode (e-APD) detector. Finally, the IPDA detected signals are digitized and stored through a state-of-the-art data acquisition units. The completed triple-pulse IPDA data acquisition software includes data reduction algorithms that is based on sample averaging, which result in virtual sampling rate reduction. In addition, work is currently focused on real time data processing that allows data storage either in raw format, processed format or both.

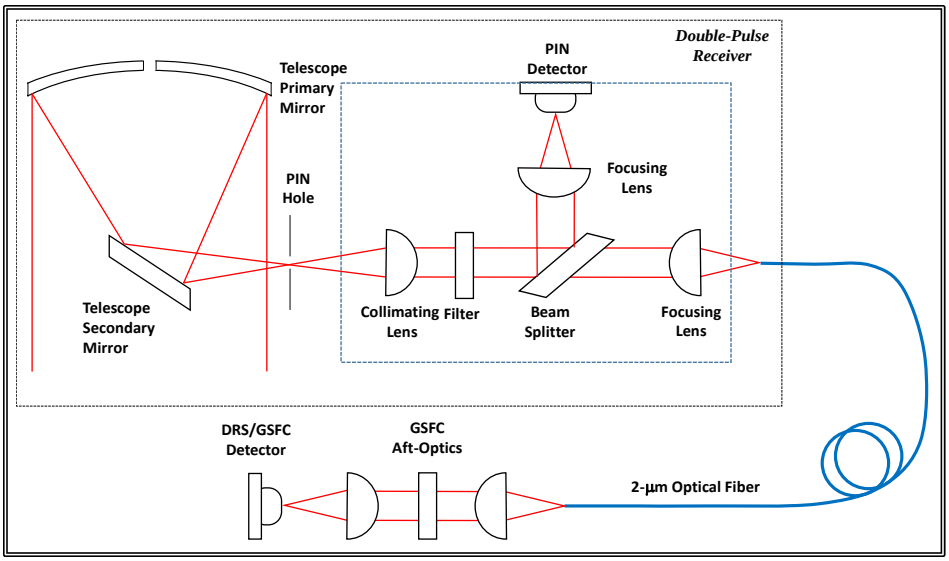

Figure 20. 2-μm triple-pulse IPDA receiver system, integrated based on the previous double-pulse system. The receiver consists of a telescope, aft optics with high-signal InGaAs channel and low-signal e-APD channel. The e-APD channel is coupled through an optical fiber through additional aft-optics.

4.1 Receiver Telescope

Similar to the double-pulse IPDA, the receiver telescope design is a Newtonian type with 0.4 m diameter aluminum primary mirror, shown in figure 11. The shape of the primary mirror is hyperbolic to minimize the aberration and focus the return signal to less than 300-μm diameter spot size. The telescope is designed to maintain the focus point position in the temperature range between 5 and 35°C. The telescope secondary mirror, shown in figure 12, is a fused silica, two surfaces, dichroic flat that turns the return radiation 90º to the side integrated aft-optics from one surface. The opposite surface is used to transmit the expanded laser beam coaxially with the telescope. A single automated mount is used for bore-sight alignment. The primary goal of the telescope integration, shown in figure 12, is to assemble the various parts without any undue stresses. The stress level, mainly due to the primary mirror weight, was measured at a wavelength accuracy and was recorded before and after the assembly. The focal point of the telescope was measured and the position was identified using a 300-μm diameter pinhole that was placed at the focal point. A simple geometric alignment procedure was established to verify consistent telescope alignment after shipping to LaRC. That included an integrated vibration monitor that was attached to the structure.

4.2 Detection Systems

Recent development of advance single-charge-carrier, HgCdTe (MCT) e-APD indicated a breakthrough in lidar detection technology [15]. These devices are space-qualifiable and were validated for airborne lidar operation at 1.6-μm at GSFC [16]. MCT e-APD are sensitive to IR radiation up to 4-μm. Therefore, a cold narrow band-pass filter is desired to limit the device background. In co-ordination with ESTO, LaRC collaborated with GSFC to integrate the detector into the triple-pulse 2-μm IPDA lidar low signal channel. This e-APD comes with 4 by 4 pixel format (80×80 μm^2 pixel area) with read-out electronics that enable access to each pixel through individual TIA. An output summing amplifier would produce the sum of specific number of pixels as selected by the operator. The detector is integrated inside a vacuum chamber, shown in figure 13, which allows cooling the device with cryo-cooler down to 70 K to reduce dark current and noise. The e-APD and readout electronics are integrated inside a rack mountable chassis, shown in figure 13, which includes vacuum circuit for thermal isolation. Additional custom designed aft-optics would allow focusing the radiation onto selected number of pixels. The e-APD custom aft-optics is coupled to the IPDA aft-optics through a 2-μm optical fiber, as shown in figure 10. Work efforts at GSFC included 2-μm cold filter integration to the detector chamber, detector assembly testing, additional aft-optics design with optical fiber coupling. Airborne detector chassis assembly and testing were conducted. Combining both the 2-μm triple-pulse transmitter with this new detection system in a single instrument will result in a CO_2 IPDA lidar with enabling technology that meets or exceeds space requirement [8].

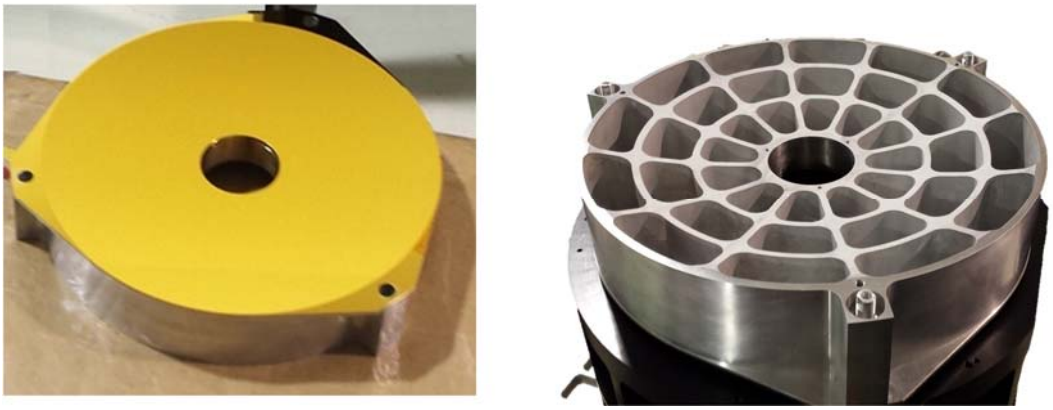

Figure 31. Front (left) and back (right) surfaces of the triple-pulse IPDA telescope primary mirror. The all-aluminum mirror structure is 40 cm in diameter, 93 focal length and weights 10.4 kg.

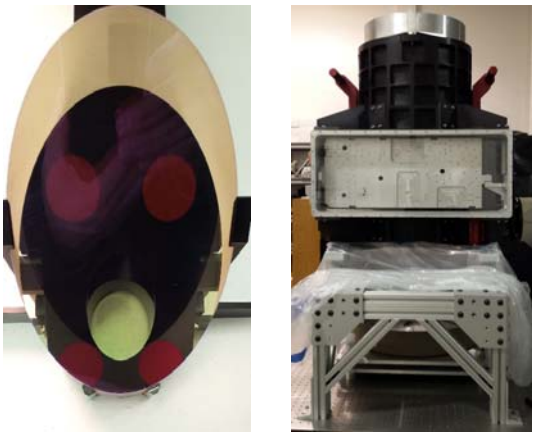

Figure 42. Triple-pulse IPDA telescope secondary mirror (left) and assembly testing (right). Both surfaces of the fused silica secondary mirror are coated for 2-μm wavelength. The front surface is used for steering the return radiation toward the aft-optics box. The back surface is used for the transmitting the output expanded laser beam coaxially with the telescope.

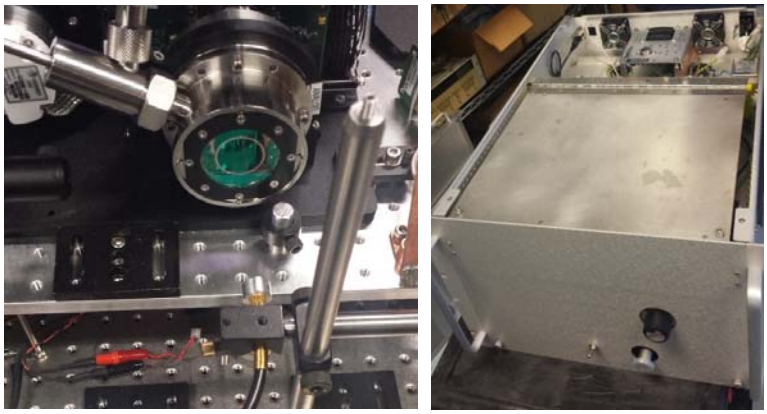

Figure 13. Triple-pulse IPDA telescope assembly testing (left) and the secondary mirror (right). Both surfaces of the fused silica secondary mirror are coated for 2-μm wavelength. The front surface is used for steering the return radiation toward the aft-optics detector box. The back surface is used for the transmitting the output laser coaxially with the telescope.

4.3 Data Acquisition System

The data acquisition unit is based on two similar high-performance digitizers (Agilent; U5303A). These are 12-bit two-channel digitizers that operate at a fixed sampling rate of 1 GS/s. These digitizers are triggered from the laser Q-switch and come with a self-calibration option that is activated for gain and offset measurement and correction for every record. One digitizer is dedicated to the IPDA hard target return signals, with a variable record length of about 70k samples, while the other is dedicated to the laser energy monitors, with a fixed record length of 10k. Using these digitizers is another major enhancement of the triple-pulse IPDA over the double-pulse. Although, digitized data have 12-bit resolution, data storage is achieved in byte increments, leading to 16-bit data record. This indicates that 25% of the recorded data would be null. Therefore, optional sample averaging take advantage of some of the extra 4-Bits, while enhancing the data record precision, lowering noise and reducing data volume, as indicated in figure 14. For example, a 1 second worth of data at 50 Hz repetition rate would results in 150 laser pulses. For each pulse, 4 records are obtained, two from two different energy monitors and another two from the two different detection channels. This would translate to 600 records. Taking into account the record length and two-byte requirement per sample would result in 48 M-Byte/sec data rate. Thus, for an average two hours flight the total data collected would be 344 GByte, at 1 GHz sampling rate. Using sampling average, this can be significantly reduced, while enhancing the noise performance, as demonstrated in figure 16. The figure presents digitizer noise measurements that were conducted with 50Ω floating input for all channels. Statistical analysis indicated less than 1 mV noise voltage (2 counts at 1GS/s), which can be reduced further with sample averaging. With 2V input range, this results in signal-to-noise ratio limit of about 2000. The digitizer's data acquisition software was compiled with LabView and output data is stored in MATLAB compatible binary files, which includes the raw data and housekeeping.

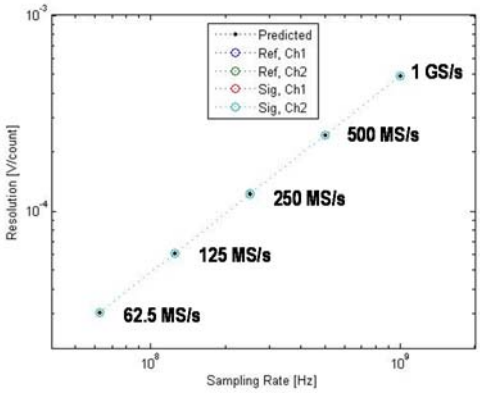

Figure 14. Measurement of the sampling resolution versus sampling rate for all four channels of the two digitizers selected for the triple-pulse IPDA liadr data acquisition. The sampling rate was reduced by sample averaging of the 1GS/s acquired data. The predicted resolution is the result of the ratio of the digitizer full scale range of 2 V to the total number of code obtained from 2N, where N is the number of bits.

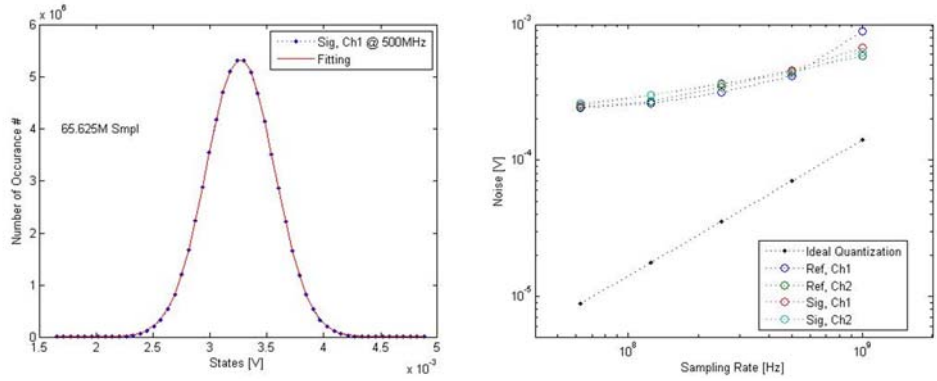

Figure 15. Digitizer noise statistics (left) and noise voltage comparison to ideal quantization error (right). Results indicates less than 1 mV noise voltage (2 counts at 1GS/s), which reduces with sample averaging. With 2V input range, this results in signal-to-noise ratio limit of about 2000.

5. VALIDATION PLANS

The 2-μm IPDA lidar validation is important to assess both CO_2 and H_2O atmospheric measurements. IPDA validation is conducted by comparing the instrument measurement to other gas sensors. Instrument validation will start on ground after instrument integration in the lidar mobile laboratory. The mobile laboratory enables IPDA lidar horizontal measurement using a set calibrated hard targets with different reflectivity, in addition to vertical measurements using clouds as hard target. The main ground validation objectives are to check IPDA operational readiness before aircraft deployment, obtain IPDA signals and noise to evaluate instrument systematic and random errors, compare instrument errors to IPDA models and compare CO_2 and H_2O measurements against correlative in-situ instruments, such as CAPABLE, radiosonde, LiCor and Piccaro. Other long term objectives include transferring the laboratory with the instrument to different tall tower sites, such as WLEF tall tower in Park Falls, Wisconsin, and the Southern Great Plains ARM site in Lamont, Oklahoma.

For airborne operation, the objective of the initial engineering flights would focus on instrument operation and comparing the airborne and ground performance related to signal and noise. Once achieved, the objective would focus on comparing CO_2 and H_2O measurements against correlative in-situ sensors and models. The validation will rely on onboard sensors (aircraft sensors, LiCor and Piccaro) as well as coordinating and collaborate with science community from other independent sensors, such as NOAA air-sampling flask flights and Pennsylvania State University passive sensors. At this stage, the main goal is to evaluate and verify both the systematic and the random errors. On the other hand, airborne validation will be planned to target different conditions such as different surface reflectivity (land, ocean, snow, sand, vegetation) uniform versus variable surface reflectivity, day and night background, clear, cloudy and broken cloud conditions, variable surface elevation and urban pollution and plume detection. The validation may also cover different location such as the Upper Midwest summer, where strong vertical and horizontal spatial gradients in CO_2 occurs due to agricultural fluxes and urban deployment in winter, where flight around isolated urban centers could identify a clear atmospheric boundary layer CO_2 plume (for example, Indianapolis, build on existing in situ observational network). Also, these 2-μm triple-pulse validation activities might have the potential to coordinate with ACT-America flights.

6. CONCLUSIONS

A 2-μm double-pulse IPDA lidar instrument have been developed at NASA LaRC. This instrument was validated for active remote sensing of carbon dioxide in the atmosphere. As an upgrade, a 2-μm triple-pulse IPDA lidar instrument is being developed at NASA LaRC. This active remote sensing IPDA instrument targets and measures both atmospheric carbon dioxide and water vapor. Wavelength selection and laser transmitter operation allows measuring both species independently and simultaneously. This would be the first demonstration of measuring two different atmospheric molecules with a single instrument. The basic instrument design is based on knowledge gathered through the previously successful 2-μm double-pulse IPDA. Critical enhancements were implemented in the new triple-pulse design that significantly advance the technology. These enhancements includes both the transmitter and receiver. For the transmitter, modifications include triple-pulse operation of the laser, laser timing control updates and wavelength control design. In the receiver, updates includes telescope integration, data acquisition system and additional high performance e-APD detector. The e-APD detector supplied by NASA GSFC, is a state-of-art, space qualifiable device that was validated for lidar applications. Combining both the 2-μm triple-pulse transmitter with this new detector in a single instrument will result in a CO_2 IPDA lidar with enabling technology, which meets or exceeds space requirements. Work progress of the 2-μm triple-pulse IPDA program is on schedule. Instrument validation plans are under discussions to collaborate with different institutes with similar interests.

ACKNOWLEDGMENTS

This work was funded and supported by NASA Earth Science Technology Office (Program Director: George Komar and Program Manager: Parminder Ghuman).

REFERENCES

[1] T. Refaat, U. Singh, J. Yu, M. Petros, R. Remus, and S. Ismail, "Double-pulse 2-μm integrated path differential absorption lidar airborne validation for atmospheric carbon dioxide measurement", Applied Optics, 55(15), 4232-4246 (2016).

[2] U. Singh, J. Yu, M. Petros, T. Refaat, R. Remusa, J. Faya and K. Reithmaier, "Airborne 2-micron double-pulsed integrated path differential absorption lidar for column CO_2 measurement", Proc. SPIE, 9246, 924602 (2014).

[3] U. Singh, T. Refaat, J. Yu, M. Petros and R. Remus, "Airborne active remote sensor for atmospheric carbon dioxide", SPIE Newsroom (2015).

[4] U. Singh, J. Yu, M. Petros, T. Refaat, R. Remus, J. Fay and K. Reithmaier, "Airborne 2-micron double-pulsed integrated path differential absorption lidar for column CO_2 measurement", Proc. SPIE 9246, 924602 (2014).

[5] U. Singh, T. Refaat, J. Yu, M. Petros and R. Remus, "Double-pulsed 2-μm lidar validation for atmospheric CO_2 measurements", Proc. SPIE 9645, 964502 (2015).

[6] U. Singh, J. Yu, M. Petros, T. Refaat, R. Remus and K. Reithmaier, "Development of double- and triple-pulsed 2-micron IPDA lidars for column CO_2 measurements", Proc. SPIE, 9612, 961204 (2015).

[7] J. Yu, M. Petros, T. Refaat, K. Reithmaier, R. Remus, U. Singh, W. Johnson, C. Boyer, J. Fay, S. Johnston, L. Murchison, "Airborne 2-micron double pulsed direct detection IPDA lidar for atmospheric CO_2 measurement", in EPJ Web of Conferences, 27th International Laser Lidar Conference, 119, 02001 (2016).

[8] U. Singh, M. Petros, T. Refaat, and J. Yu, "2-micron triple-pulse integrated path differential absorption lidar development for simultaneous airborne column measurements of carbon dioxide and water vapor in the atmosphere", Proc. SPIE, 9879, 987902 (2016).

[9] T. Refaat, U. Singh, J. Yu, M. Petros, S. Ismail, M. Kavaya, and K. Davis, "Evaluation of an airborne triple-pulsed 2-μm IPDA lidar for simultaneous and independent atmospheric water vapor and carbon dioxide measurements", Applied Optics, 54(6), 1387-1398 (2015).

[10] U. Singh, B. Walsh, J. Yu, M. Petros, M. Kavaya, T. Refaat, and N. Barnes, "Twenty years of Tm:Ho:YLF and LuLiF laser development for global wind and carbon dioxide active remote sensing", Optical Materials Express, 5(4), 827-837 (2015).

[11] U. Singh, T. Refaat, M. Petros, and J. Yu, "Triple-pulse two-micron integrated path differential absorption lidar: a new active remote sensing capability with path to space", in EPJ Web of Conferences, 27th International Laser Lidar Conference, 119, 02001 (2016).

[12] T. Refaat, U. Singh, M. Petros, R. Remus and J. Yu, "Self-calibration and laser energy monitor validation for a double-pulsed 2-μm CO_2 integrated path differential absorption lidar application", Applied Optics, 54(24), 7240-7251 (2015).

[13] T. Refaat, M. Petros, R. Remus, J. Yu, and U. Singh, "Laser energy monitor for double-pulsed 2-μm IPDA lidar application", Proc. SPIE, 9246, 924606 (2014).

[14] M. Bagheri, G. Spiers, C. Frez, S. Forouhar, and F. Aflatouni, "Linewidth measurement of distributed-feedback semiconductor lasers operating near 2.05 μm," IEEE Photonics Technology Letters, 27(18), 1934-1937 (2015).

[15] T. Refaat, M. Petros, C. Antill, U. Singh, and J. Yu, "Wavelength locking to CO_2 absorption line-center for 2-μm pulsed IPDA lidar application", Proc. SPIE, 9879, 987904 (2016).

[16] J. Beck, T. Welch, P. Mitra, K. Reiff, X. Sun, and J. Abshire, "A highly sensitive multi-element HgCdTe e-APD detector for IPDA lidar applications", Journal of Electronic Materials, 43(8), 2970-2977 (2014).

[17] X. Sun, J. Abshire, and J. Beck, "HgCdTe e-APD detector arrays with single photon sensitivity for space lidar applications", Proc. SPIE, 9114, 91140K (2014).